ARTHRITIS & RHEUMATOLOGY
Vol. 68, No. 12, December 2016, pp 2975–2985
DOI 10.1002/art.39828

Histone Deacetylase 5 Is Overexpressed in Scleroderma Endothelial Cells and Impairs Angiogenesis via Repression of Proangiogenic Factors

Pei-Suen Tsou,[1] Jonathan D. Wren,[2] M. Asif Amin,[1] Elena Schiopu,[1] David A. Fox,[1] Dinesh Khanna,[1] and Amr H. Sawalha[1]

Objective. **Vascular dysfunction represents a disease-initiating event in systemic sclerosis (SSc; scleroderma). Results of recent studies suggest that epigenetic dysregulation impairs normal angiogenesis and can result in abnormal patterns of blood vessel growth. Histone deacetylases (HDACs) control endothelial cell (EC) proliferation and regulate EC migration. Specifically, HDAC-5 appears to be antiangiogenic. This study was undertaken to test whether HDAC-5 contributes to impaired angiogenesis in SSc by repressing proangiogenic factors in ECs.**

Methods. **Dermal ECs were isolated from patients with diffuse cutaneous SSc and healthy controls. Angiogenesis was assessed using an in vitro Matrigel tube formation assay. An assay for transposase-accessible chromatin using sequencing (ATAC-seq) was performed to assess and localize the genome-wide effects of *HDAC5* knockdown on chromatin accessibility.**

Results. **The expression of *HDAC5* was significantly increased in ECs from patients with SSc compared to healthy control ECs. Silencing of *HDAC5* in SSc ECs restored normal angiogenesis. *HDAC5* knockdown followed by ATAC-seq assay in SSc ECs identified key *HDAC5*-regulated genes involved in angiogenesis and fibrosis, such as *CYR61*, *PVRL2*, and *FSTL1*. Simultaneous knockdown of *HDAC5* in conjunction with either *CYR61*, *PVRL2*, or *FSTL1* inhibited angiogenesis in SSc ECs. Conversely, overexpression of these genes individually led to an increase in tube formation as assessed by Matrigel assay, suggesting that these genes play functional roles in the impairment of angiogenesis in SSc.**

Conclusion. **Several novel *HDAC5*-regulated target genes associated with impaired angiogenesis were identified in SSc ECs by ATAC-seq. The results of this study provide a potential link between epigenetic regulation and impaired angiogenesis in SSc, and identify a novel mechanism for the dysregulated angiogenesis that characterizes this disease.**

Systemic sclerosis (SSc; scleroderma) is a poorly understood autoimmune disease that is characterized by vascular injury and debilitating tissue fibrosis. Activation of endothelial cells (ECs) and inflammatory cells, as well as fibroblasts, leads to excessive production of extracellular matrices, which accumulate in various organs. Widespread vascular damage appears to be an early disease event, as morphologic changes in the vasculature occur before the onset of tissue fibrosis. This is supported by the early presentation of Raynaud's phenomenon, a condition that occurs as the first symptom in almost all patients with SSc, prior to the occurrence of fibrosis. Other vascular complications include pulmonary arterial hypertension and scleroderma renal crisis, both of which contribute significantly to mortality in SSc (1).

In the skin, SSc vasculopathy leads to loss of dermal capillaries, resulting in tissue hypoxia and ischemia, which, under normal circumstances, prompts angiogenesis.

Supported by the NIH (National Institute of Arthritis and Musculoskeletal and Skin Diseases grants T32-AR-007080 to Dr. Tsou and K24-AR-063120 to Dr. Khanna, National Institute of Allergy and Infectious Diseases grants UM1-AI-110557 to Dr. Fox, UM1-AI-110557 to Dr. Khanna, and R01-AI-097134 and U19-AI-110502 to Dr. Sawalha, and grant P20-GM-103636 to Dr. Wren). Dr. Tsou's work was also supported by the Scleroderma Foundation.

[1]Pei-Suen Tsou, PhD, M. Asif Amin, MD, Elena Schiopu, MD, David A. Fox, MD, Dinesh Khanna, MD, MSc, Amr H. Sawalha, MD: University of Michigan, Ann Arbor; [2]Jonathan D. Wren, PhD: Oklahoma Medical Research Foundation and University of Oklahoma Health Sciences Center, Oklahoma City.

Address correspondence to Amr H. Sawalha, MD, Division of Rheumatology, University of Michigan, 1150 West Medical Center Drive, 5520 MSRB1, SPC 5680, Ann Arbor, MI 48109. E-mail: asawalha@umich.edu.

Submitted for publication January 25, 2016; accepted in revised form July 26, 2016.

However, in SSc, this compensatory process is impaired and the ECs are incapable of building new blood vessels (2). The mechanism of dysregulated angiogenesis in SSc ECs appears to be multifactorial. These mechanistic factors include altered expression of angiogenic-related proteins and transcription factors (2–4), impairment of the urokinase-type plasminogen activator receptor pathway (2), defects in the basic fibroblast growth factor (bFGF) and vascular endothelial growth factor (VEGF) pathways (2,5–7), and changes in chemokine and chemokine receptor expression and signaling (2,4,8). In addition, SSc ECs can promote fibroblast activation via the CCN2/transforming growth factor β (TGFβ) pathway (9). Epigenetic mechanisms of SSc EC dysfunction have also been noted, as evidenced by the fact that the lower expression of bone morphogenetic protein receptor type II in these cells can be modified by inhibitors of DNA methyltransferase and histone deacetylase (HDAC) (10).

Emerging data on the role of epigenetics in angiogenesis are beginning to shed light on the effects of abnormal angiogenesis in different diseases. Specifically, HDACs, which enzymatically remove acetyl groups from histones, appear to play significant roles in blood vessel formation. It was reported that nonselective inhibitors of HDACs reduce tube formation of ECs in vitro, inhibit postnatal neovascularization in response to hypoxia, and block tumor angiogenesis (11). Moreover, the enzymatic activity of class I and class II HDACs is essential for endothelial commitment of progenitor cells (11). Studies in which individual HDACs were examined in ECs revealed that class IIa HDACs (HDAC-5, HDAC-7, and HDAC-9), class IIb HDACs (HDAC-6), and class III HDACs (SIRT-1) are involved in angiogenesis (11). They have been shown to affect endothelial functions, including EC proliferation, migration, and apoptosis. Among them, HDAC-5 is antiangiogenic, since knockdown of *HDAC5* messenger RNA (mRNA) resulted in EC migration and sprouting (12). It appears that *HDAC5* represses a number of angiogenic genes, such as *SLIT2* (gene for Slit homolog 2 protein) and *FGF2* (gene encoding fibroblast growth factor 2; also known as bFGF), by binding to their promoter region (12).

In this study, we examined the role of HDAC-5 in impaired angiogenesis in SSc ECs. We first examined the expression of *HDAC5* in ECs isolated from healthy volunteers or patients with diffuse cutaneous SSc, and assessed whether knockdown of *HDAC5* mRNA in SSc ECs would alter their angiogenic ability. We then utilized an unbiased approach to assess chromatin accessibility and identify target genes repressed by *HDAC5* in ECs, followed by bioinformatics analyses and experimental validation of the identified targets. Several *HDAC5*-regulated genes that play a critical role in dysregulated angiogenesis in SSc were identified.

PATIENTS AND METHODS

Patients. All patients met the American College of Rheumatology/European League Against Rheumatism criteria for the classification of SSc (13). The demographics and clinical characteristics of the enrolled patients are summarized in Table 1. Two 4-mm punch biopsy specimens from the distal forearm of healthy volunteers and patients with diffuse cutaneous SSc were obtained for EC isolation. All subjects included in this study signed a written informed consent. All procedures in this study were reviewed and approved by the Institutional Review Board of the University of Michigan.

Cell culture. Dermal ECs were isolated and characterized in our laboratory in a manner as previously described (4,6). After digestion, ECs were purified using a CD31 MicroBead kit and a MiniMACS Separator with an MS Column (Miltenyi Biotech), and grown in EBM-2 medium with growth factors (Lonza). Cells between passages 3 and 6 were used in the experiments.

Extraction of mRNA and quantitative polymerase chain reaction (qPCR). Total RNA from cells was isolated using a Direct-zol RNA MiniPrep kit (Zymo Research) or RNeasy Mini kit (Qiagen). A Verso complementary DNA (cDNA) synthesis kit was used to prepare cDNA (Thermo Scientific). Primers for human *HDAC4, HDAC5, HDAC6, HDAC7, HDAC9, HDAC10, VEGF*, and *β-actin*, along with Power SYBR Green PCR Master Mix (Applied Biosystems), were applied for qPCR, which was run using either a ViiA 7 Real-Time PCR system or an Applied Biosystems Real-Time PCR system. Primer sequences are as follows: for *HDAC4*, forward TGTACGACGCCAAAGATGAC and reverse CGGTTCAGAAGCTGTTTTCC; for *HDAC5*, forward CAGCAGGCGTTCTACAATGA and reverse CGATGCAGAGAGATGTAGAGCA; for *HDAC6*, forward GAAAGTCACCTCGGCATCAT and reverse TAGTCTGGCCTGGAGTGGAC; for *HDAC7*, forward ATGGGGGATCCTGAGTACCT and reverse GATGGGCATCACGACTATCC; for *HDAC9*, forward CTGGAGCCCATCTCACCTT and reverse TCATCATCCTGAGGTC-

Table 1. Characteristics of the patients with diffuse cutaneous systemic sclerosis (SSc) and healthy controls

	Patients with SSc (n = 12)	Healthy volunteers (n = 8)
Age, mean ± SEM years	50.9 ± 4.2	49.8 ± 5.0
Sex, no. female/no. male	10/2	6/2
Disease duration, mean ± SEM years	3.4 ± 0.7	NA*
Modified Rodnan skin thickness score, mean ± SEM†	14.3 ± 2.6	NA
Raynaud's phenomenon, no.	12	NA
Early disease (<5 years), no.	10	NA
Digital ulcers, no.	2	NA
Telangiectasias, no.	7	NA
Gastrointestinal disease, no.	9	NA
Interstitial lung disease, no.	9	NA
Pulmonary arterial hypertension, no.	4	NA
Renal involvement, no.	1	NA

* NA = not applicable.
† Maximum possible score 51.

TGTCC; for *HDAC10*, forward GCCGGATATCACATTGGTTC and reverse GACGCTTCCTGTTGGATGA; for *VEGF*, forward ATGAACTTTCTGCTGTCTTGGGT and reverse TGGCCTTG-GTGAGGTTTGATCC; and for *β-actin*, forward GTCAGGCA-GCTCGTAGCTCT and reverse GCCATGTACGTTGCTAT-CCA. The rest of the primers were KiCqStart SYBR Green primers from Sigma.

Western blots. Cell lysates were obtained both from healthy subjects and from patients with SSc. Equal amounts of protein were separated by sodium dodecyl sulfate–polyacrylamide gel electrophoresis and electroblotted onto nitrocellulose membranes. HDAC-5 proteins were detected using anti-human HDAC-5 antibodies (Cell Signaling Technology), while β-actin was used as a loading control (anti–β-actin antibodies were from Sigma-Aldrich). Band quantification was performed using GelQuant.NET (BiochemLab Solutions).

Gene knockdown experiments. To evaluate the effect of HDAC-5 on angiogenesis in SSc ECs, its expression was knocked down using *HDAC5* small interfering RNA (siRNA) (Santa Cruz Biotechnology), while a nontargeted siRNA (Life Technologies) was used as a control. We first utilized ECs from healthy subjects to establish the transfection condition. ECs were transfected with 25–75 n*M* of siRNA using TransIT-TKO transfection reagent (Mirus Bio) for 48 hours, and mRNA/protein lysates were collected. We then confirmed the knockdown of *HDAC5* using SSc ECs. The knockdown condition was also optimized for experiments using *PVRL2* siRNA (50 n*M*), *CTNNAL1* siRNA (50 n*M*), *FSTL1* siRNA (25 n*M*), and *FSTL3* siRNA (25 n*M*) (all from Santa Cruz Biotechnology), as well as siRNA for *ID2* (150 n*M*) and *CYR61* (25 n*M*) (both from GE Dharmacon).

Gene overexpression experiments. Induction of overexpression of *PVRL2*, *FSTL1*, and *CYR61* was performed as previously described, with some modifications (4). ECs were transfected with 0.33 μg of *FSTL1* or *PVRL2* (or control vector pCMV6-XL5) or 1.65 μg of *CYR61* (or control vector pCMV6-XL4) (all from Origene) and Lipofectamine 2000 (Invitrogen) for 24 hours in T12.5 flasks. Five hours after transfection, the culture medium was changed to allow the cells to grow in endothelial growth medium supplemented with bovine brain extract (Lonza). Thereafter, qPCR analyses or Matrigel tube formation assays were performed.

Enzyme-linked immunosorbent assay (ELISA). The levels of VEGF and bFGF in cell culture supernatants were measured using ELISA kits (R&D Systems). The absorbance of each well was read using a microplate reader at 450 nm.

Matrigel tube formation assay. A Matrigel tube formation assay was performed to evaluate the effect of HDAC-5 on angiogenesis (6). Transfected SSc ECs were suspended in EBM-2 medium with 0.1% fetal bovine serum and plated in 8-well Lab-Tek chambers coated with growth factor–reduced Matrigel (BD Biosciences). The cells were fixed and stained after overnight incubation. Quantitation of the tubes formed by ECs was performed in a blinded manner by a researcher (MAA). Pictures of each well were taken using an EVOS XL Core Cell Imaging system (Life Technologies). In the double-knockdown study, SSc ECs were transfected for 48 hours with control siRNA, *HDAC5* siRNA, or *HDAC5* plus the siRNA for genes of interest, and then plated on Matrigel. For the overexpression experiments, SSc ECs were transfected with control vector, *FSTL1*, *PVRL2*, or *CYR61* and the Matrigel assay was carried out the next day.

Assay for transposase-accessible chromatin using sequencing (ATAC-seq). To characterize the impact of *HDAC5* knockdown on chromatin accessibility at a genome-wide level, ATAC-seq was performed (14). This utilizes a hyperactive Tn5 transposase that simultaneously cuts and ligates adaptors at regions of open chromatin. Since *HDAC5* knockdown alters the chromatin structure, application of ATAC-seq in this study allowed us to assess genome-wide chromatin accessibility in SSc ECs with a high degree of accuracy and sensitivity. After transfection, 50,000 ECs were collected and lysed in 50 μl lysing buffer (10 m*M* Tris HCl, pH 7.4, 10 m*M* NaCl, 3 m*M* $MgCl_2$, 0.1% Igepal CA-630). After centrifugation, the supernatant was discarded and the pellet was used for transposition. The transposition reaction included 25 μl 2 × TD buffer (Illumina), 2.5 μl Tn5 transposase (Illumina), and 22.5 μl water. The mixture was incubated at 37°C for 30 minutes. After purification, DNA libraries were prepared by PCR and purified using a Qiagen MinElute kit. To assess the quality of the DNA libraries, gel electrophoresis was performed and the DNA was visualized using Omega Lum C (Aplegen). Libraries that passed quality control measures, as previously described (14), were sequenced with 50-bp pair-end reads on an Illumina Hi-Seq 2500 platform (3 samples per lane).

ATAC-seq data analysis. Sequencing reads were aligned to the human genome assembly (hg19) using Burrows-Wheeler Alignment (version 0.7.5) (15). Improperly paired alignment and alignment with a mapping quality of <4 were filtered using SAMtools (version 0.1.19) (16). Peak-calling was then performed using MACS2 (version 2.0.10) (17), with reads shifted and extended by the parameters "–nomodel –shift -100 –extsize 200 -B –broad". Blacklisted genomic regions (18) were removed from the peaks. Comparison of the findings in the cells under each knockdown condition (*HDAC5* knockdown versus control siRNA treatment) was performed using diffReps (version 1.55.4) (19), with the 3 individual experiments treated as triplicates for each condition. Running diffReps with a negative binomial model and a *P* value threshold of 1×10^{-4} identified peaks that had significantly different signal abundance (at a significance level of $P < 0.05$) between the 2 conditions, after adjustment with the Benjamini-Hochberg method.

Bioinformatics analysis. To identify genes that are relevant to SSc, genes that showed differential chromatin accessibility after *HDAC5* knockdown in ECs were subjected to bioinformatics analysis using IRIDESCENT (20). This analysis searches for co-occurrence of the genes and the key words (i.e., fibrosis or angiogenesis) within the scientific literature. A statistical method was used to score the relevance of the co-occurrence by comparing the observed frequencies to those randomly occurring by chance (20).

Statistical analysis. Results are expressed as the mean ± SD. To determine the differences between the groups (as shown in Figure 1), Mann-Whitney U test was performed using GraphPad Prism version 6. To compare the biomarkers in SSc ECs under each transfection condition (*HDAC5* knockdown versus control siRNA treatment) (as shown in Table 3), a paired *t*-test was performed. *P* values less than 0.05 were considered statistically significant.

RESULTS

Aberrant expression of class II HDACs in SSc ECs. We examined the expression of class IIa and class IIb HDACs using qPCR. As shown in Figure 1A,

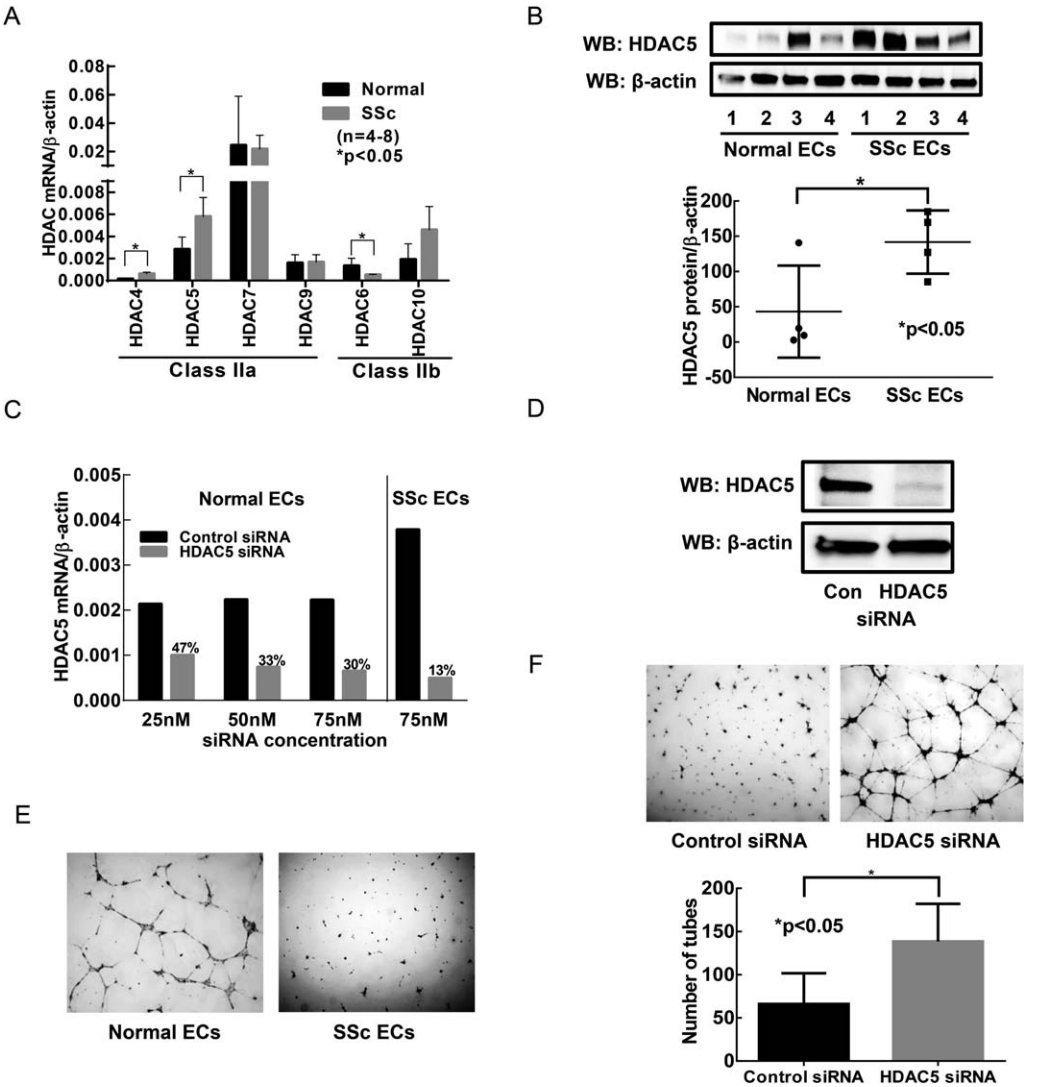

Figure 1. Effect of histone deacetylase 5 (HDAC-5) expression on the angiogenic ability of endothelial cells (ECs) from patients with systemic sclerosis (SSc). **A,** Expression of class IIa and class IIb *HDAC*s in SSc ECs compared to healthy control ECs. **B,** Determination of HDAC-5 protein levels by Western blotting (WB) (top) and quantification of HDAC-5 protein levels (bottom) in SSc ECs compared to healthy control ECs. Symbols represent individual cell samples; bars show the mean ± SD. **C,** Effects of knockdown of *HDAC5* mRNA in healthy control ECs (utilizing varying concentrations of *HDAC5* small interfering RNA [siRNA]) and in SSc ECs (utilizing 75 n*M HDAC5* siRNA), as compared to control siRNA treatment. **D,** Confirmation, at the protein level, of HDAC-5 knockdown by *HDAC5* siRNA, in contrast to control (Con) siRNA treatment. **E,** Evaluation of tube formation on Matrigel assay in SSc ECs compared to healthy control ECs, showing the antiangiogenic nature of SSc ECs. **F,** Effects of *HDAC5* knockdown on tube formation in SSc ECs, as shown on Matrigel assay (top) and quantified according to the number of tubes formed (bottom) in *HDAC5* siRNA–treated cells compared to control siRNA–treated cells. Results are the mean ± SD in 4–8 cell samples in **A** and **C** and 5 cell samples in **F.** The experiments utilized β-actin as a loading control.

expression of *HDAC4* and *HDAC5*, both class IIa HDACs, was up-regulated in SSc ECs compared to healthy control ECs, whereas expression of *HDAC6*, a class IIb HDAC, was down-regulated (each $P < 0.05$). We further confirmed the increased expression of HDAC-5 in SSc ECs at the protein level (Figure 1B). Although HDAC-5 expression was variable among SSc patients, its expression was significantly increased in all SSc ECs ($n = 4$; $P < 0.05$ versus healthy controls).

Since HDAC-5 is antiangiogenic, we proceeded to knock down *HDAC5* mRNA in ECs and examined whether the decrease in *HDAC5* expression altered the angiogenic ability of SSc ECs. We first established the optimal *HDAC5* knockdown condition (Figure 1C). In

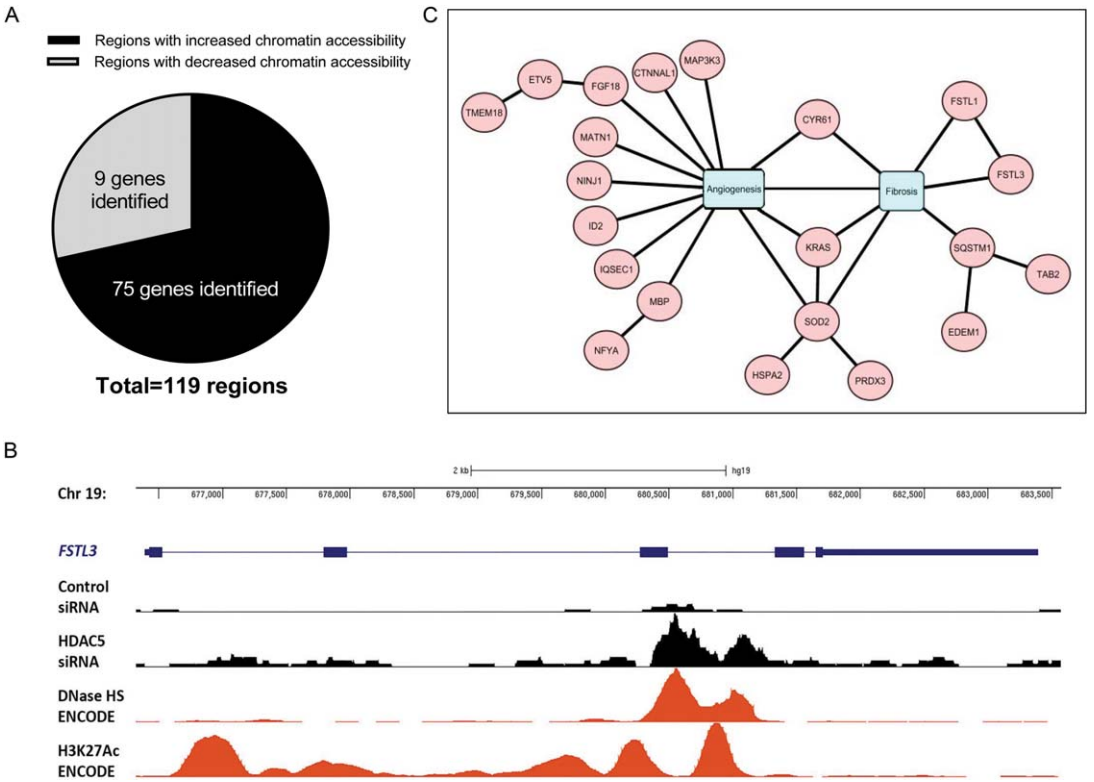

Figure 2. Differential open-chromatin regions revealed by transposase-accessible chromatin using sequencing (ATAC-seq) assay after *HDAC5* knockdown in endothelial cells (ECs) from patients with systemic sclerosis (SSc). **A,** Increased chromatin accessibility after *HDAC5* knockdown, compared to control small interfering RNA (siRNA) transfection, in SSc ECs. With a cutoff value of 20% established for change in chromatin accessibility and a *P* value of <0.05 (adjusted for multiple testing), a total of 119 regions were identified (85 regions with increased chromatin accessibility, and 34 regions with decreased chromatin accessibility). In the regions of increased chromatin accessibility, 75 genes were located in these sites and only 9 genes were located in less-accessible regions. **B,** University of California, Santa Cruz Genome Browser tracks of the *FSTL3* locus along with data from ATAC-seq analysis of signals from control siRNA–treated or *HDAC5* siRNA–treated samples, DNase I hypersensitivity (HS) mapping from human umbilical endothelial cells (HUVECs) (generated by the ENCODE project), and ChIP-seq data on H3K27Ac in HUVECs (from the ENCODE project). *HDAC5* knockdown resulted in an increase in peak intensity compared to control siRNA treatment. The ATAC-seq signals were very similar to the DNase I hypersensitivity sequencing and overlapped H3K27Ac enrichment in HUVECs. **C,** IRIDESCENT analysis of genes located in the more-accessible chromatin regions after *HDAC5* knockdown, to identify genes that were related to angiogenesis or fibrosis in SSc ECs.

healthy donor ECs, 75 n*M* of *HDAC5* siRNA resulted in ~70% knockdown of *HDAC5* when compared to cells transfected with control siRNA. We then used this condition in SSc ECs and achieved ~87% knockdown of *HDAC5*. Furthermore, in SSc ECs under this transfection condition, we confirmed that, at the protein level, HDAC-5 was indeed negligible (Figure 1D). Therefore, in subsequent experiments, the condition utilized for *HDAC5* knockdown was a concentration of 75 n*M* siRNA for 48 hours.

Increase in tube formation following *HDAC5* knockdown in SSc ECs. We then used a Matrigel tube formation assay to test whether a decrease in *HDAC5* expression altered the angiogenic ability of SSc ECs. We first used ECs isolated from healthy subjects and from patients with SSc and performed a Matrigel tube formation assay. Similar to findings reported previously (3,5,7), SSc ECs, in the absence of an angiogenic stimulus, were unable to form tube-like structures on Matrigel, whereas healthy donor ECs exhibited tube formation (Figure 1E). SSc ECs transfected with control siRNA also demonstrated a diminished capability to form tubes (Figure 1F). In contrast, knocking down *HDAC5* restored the ability of SSc ECs to form tubes and resulted in an ~2-fold increase in the number of tubes formed ($P < 0.05$ versus control siRNA–treated cells).

Differential open-chromatin regions revealed by ATAC-seq after *HDAC5* knockdown in SSc ECs. *HDAC5* knockdown in SSc ECs showed that chromatin accessibility was increased when compared to that in SSc ECs treated with control siRNA (Figure 2A). A total of 119 regions were identified as having at least a 20% fold difference in chromatin accessibility (≥1.2-fold or ≤0.80-fold change in sequencing peak intensity; adjusted

Table 2. Genes located in regions with at least a 1.5-fold increase in chromatin accessibility following *HDAC5* knockdown*

Chr.	Position	Gene	Fold change in peak intensity with *HDAC5* siRNA vs. control siRNA	*P*	Adjusted *P*
19	680601–681600	*FSTL3*	2.17	9.32×10^{-6}	8.14×10^{-4}
7	156930501–156931700	*UBE3C*	1.93	2.96×10^{-6}	3.57×10^{-4}
13	52979801–52980900	*THSD1*	1.84	1.54×10^{-6}	2.48×10^{-4}
21	47604401–47605600	*C21orf56*	1.83	2.43×10^{-6}	3.32×10^{-4}
1	156697701–156698700	*RRNAD1*	1.77	8.04×10^{-5}	3.91×10^{-3}
12	9066701–9067700	*PHC1*	1.75	4.40×10^{-6}	4.95×10^{-4}
11	134122401–134124000	*THYN1*	1.73	3.93×10^{-6}	4.49×10^{-4}
17	77070501–77071500	*ENGASE*	1.73	6.03×10^{-5}	3.26×10^{-3}
14	96570401–98571900	NA†	1.72	1.61×10^{-6}	2.48×10^{-4}
3	120169201–120170200	*FSTL1*	1.65	1.09×10^{-5}	9.27×10^{-4}
3	49058601–49059800	*NDUFAF3*	1.64	2.04×10^{-6}	3.08×10^{-4}
6	74363001–74364300	*SLC17A5*	1.62	2.79×10^{-5}	1.93×10^{-3}
2	238600001–238601100	*LRRFIP1*	1.61	1.13×10^{-5}	9.53×10^{-4}
5	179233401–179234700	*SQSTM1*	1.61	2.70×10^{-6}	3.49×10^{-4}
1	86045601–86047200	*CYR61*	1.60	2.31×10^{-6}	3.27×10^{-4}
17	61698601–61699700	*MAP3K3*	1.60	8.41×10^{-6}	7.55×10^{-4}
17	38108801–38109900	NA†	1.59	9.42×10^{-5}	4.43×10^{-3}
19	45348901–45349900	*PVRL2*	1.57	2.79×10^{-6}	3.49×10^{-4}
2	26256501–26257700	*RAB10*	1.56	9.68×10^{-5}	4.45×10^{-3}
5	40834901–40835900	*RPL37*	1.56	8.95×10^{-5}	4.25×10^{-3}
12	109219701–109220800	*SSH1*	1.55	3.23×10^{-5}	2.14×10^{-3}
2	112811101–112812900	*TMEM87B*	1.54	2.56×10^{-5}	1.85×10^{-3}
7	105752501–105753600	*SYPL1*	1.54	1.19×10^{-5}	9.77×10^{-4}
9	95895401–95896500	*NINJ1*	1.54	2.45×10^{-6}	3.32×10^{-4}
6	160114401–160115600	*SOD2*	1.53	2.74×10^{-6}	3.49×10^{-4}
9	77702101–77703100	*C9orf95*	1.53	2.28×10^{-6}	3.27×10^{-4}
11	112096901–112098000	*PTS*	1.52	8.11×10^{-6}	7.37×10^{-4}
12	22696601–22697600	*KIAA0528*	1.52	8.08×10^{-5}	3.91×10^{-3}
20	57267501–57268600	*NPEPL1*	1.52	2.22×10^{-4}	9.74×10^{-3}
1	171710501–171711500	*VAMP4*	1.51	3.49×10^{-5}	2.27×10^{-3}

* Chr. = chromosome; siRNA = small interfering RNA.
† Not applicable (NA) because there were no genes in this region.

$P < 0.05$). Of those identified, 85 regions showed increased chromatin accessibility, and 34 regions showed decreased chromatin accessibility. In the regions of increased chromatin accessibility, we identified a total of 75 genes located in these sites (Figure 2A). In contrast, only 9 genes were located in less-accessible regions. The genes that were located in the regions identified as more accessible to chromatin and having a 1.5-fold increase in peak intensity after *HDAC5* knockdown, relative to control siRNA treatment, are listed in Table 2.

As shown in Figure 2B (depicting genome tracks of the *FSTL3* locus), knockdown of *HDAC5* in SSc ECs increased the chromatin accessibility of *FSTL3*, as indicated by the increase in peak intensity as compared to that in control siRNA–treated cells. For validation, we compared our ATAC-seq data with chromatin-accessibility data sets such as DNase-seq. The ATAC-seq peaks correlated with DNase hypersensitivity regions generated in human umbilical vein ECs (generated by the University of Washington ENCODE group). In addition, we observed that our ATAC-seq data aligned with ChIP-seq peaks from the ENCODE project (21) for histone marks associated with active chromatin (H3K27Ac).

Up-regulation of genes involved in angiogenesis or fibrosis after *HDAC5* knockdown. Bioinformatics analysis using IRIDESCENT revealed that among the genes that were located in the regions of increased chromatin accessibility in SSc ECs after *HDAC5* knockdown, at least 16 genes appeared to be involved in angiogenesis and a few appeared to be involved in fibrosis (Figure 2C). Three genes were identified as possibly involved in both angiogenesis and fibrosis (*CYR61*, *KRAS*, and *SOD2*). We then examined the expression of these genes in SSc ECs under conditions of *HDAC5* knockdown compared to control siRNA treatment. We found that 8 genes were significantly up-regulated after *HDAC5* knockdown ($P < 0.05$) (Table 3). These included *ID2*, *CTNNAL1*, *MBP*, *PVRL2*, *CYR61*, *FSTL1*, *FSTL3*, and *SQSTM1*.

Table 3. Candidate gene mRNA expression levels after *HDAC5* knockdown compared to control siRNA treatment in endothelial cells from patients with systemic sclerosis*

Gene	Fold change in mRNA expression with *HDAC5* siRNA vs. control siRNA	*P*
ID2	2.188 ± 1.002	0.02
CTNNAL1	2.064 ± 0.880	0.03
MBP	4.073 ± 5.550	0.03
PVRL2	3.091 ± 1.600	0.02
CYR61	2.423 ± 1.562	0.03
FSTL1	2.542 ± 1.514	0.04
FSTL3	4.586 ± 4.358	0.03
SQSTM1	2.080 ± 1.419	0.04
KRAS	1.884 ± 1.250	0.08
SOD2	3.446 ± 2.591	0.08
NINJ1	1.849 ± 1.469	0.55
THSD1	1.762 ± 1.106	0.43
FGF18	1.023 ± 1.576	0.35
FAM198	1.086 ± 0.793	0.86
TAB2	1.532 ± 1.017	0.75
TMEM18	1.339 ± 0.688	0.99
IQSEC1	1.301 ± 0.661	0.22
NFYA	1.757 ± 1.622	0.19
ETV5	2.453 ± 2.228	0.83
EDEM1	1.342 ± 0.685	0.35
HSF2	1.807 ± 1.062	0.14
MAP3K3	1.417 ± 0.898	0.55
PRDX3	1.365 ± 0.664	0.31
HSPA2	1.152 ± 0.720	0.31
MATN1	ND	–

* Values are the mean ± SD change in mRNA expression in 7 pairs of endothelial cells from patients with systemic sclerosis treated with *HDAC5* small interfering RNA (siRNA) relative to control siRNA. ND = not detected.

In addition to the genes identified by ATAC-seq, we also examined the expression of 2 proangiogenic factors, VEGF and bFGF, in SSc ECs. As shown in Figure 3A, levels of mRNA for both VEGF and bFGF were significantly up-regulated after *HDAC5* knockdown. We also observed a 1.5-fold to 2-fold increase in protein levels of both VEGF and bFGF in culture supernatants of SSc ECs after *HDAC5* knockdown (data not shown).

Identification of genes that play functional roles in *HDAC5*-mediated angiogenesis. We performed double-knockdown experiments to identify genes that led to an increase in tube formation after *HDAC5* knockdown. We chose angiogenic genes that were significantly up-regulated after *HDAC5* knockdown, as listed in Table 3. These included *ID2*, *CTNNAL1*, *PVRL2*, and *CYR61*. In addition, *FSTL1* and *FSTL3* were also included, since, upon a comprehensive literature search, we determined that they appeared to be proangiogenic. *MBP* was excluded because we were unable to identify its role in angiogenesis. As shown in Figure 3B, in SSc ECs, when the expression of *FSTL1*, *PVRL2,* or *CYR61* was knocked down together with the expression of *HDAC5*, the number of tubes formed on Matrigel decreased, whereas transfection of the cells with *FSTL3*, *CTNNAL1*, or *ID2* siRNA had minimal effect, suggesting that *HDAC5* mediates its antiangiogenic effect, at least in part, through alterations in the chromatin accessibility of *FSTL1*, *PVRL2,* and *CYR61*. To further confirm their roles, we overexpressed *FSTL1*, *PVRL2*, or *CYR61* individually in SSc ECs. We found that increased expression of these genes led to an increase in the angiogenic ability of SSc ECs (Figure 3C).

DISCUSSION

In this study, we identified a novel epigenetic mechanism that contributes to the inhibition of angiogenesis in SSc. *HDAC5*, which was overexpressed in SSc ECs, inhibited angiogenesis by repressing proangiogenic genes. This was demonstrated by applying an ATAC-seq assay to assess changes in the chromatin state after *HDAC5* knockdown, thereby identifying key genes located in regions with increased chromatin accessibility. Several angiogenic and fibrosis-related genes were pinpointed on the basis of our findings, which revealed significantly increased expression of these genes after *HDAC5* knockdown. Among the proangiogenic genes identified by ATAC-seq assay, we showed that *PVRL2*, *FSTL1*, and *CYR61* played critical roles in promoting angiogenesis in SSc ECs, since overexpression of these genes resulted in increased tube formation by SSc ECs, while knocking down these genes, in conjunction with knockdown of *HDAC5*, led to decreased tube formation.

It is apparent that epigenetic changes are involved in SSc vasculopathy, since the results showed that HDAC-5 was involved in impaired angiogenesis in SSc ECs. Indeed, our results complement the findings from studies of fibrosis, in which it was shown that histone acetylation patterns differed in SSc patients, and that the use of HDAC inhibitors showed promising antifibrotic effects both in vivo and in vitro (22,23). However, global inactivation of HDACs by nonspecific inhibitors may affect angiogenesis by modifying both pro- and antiangiogenic HDACs. These pan-HDAC inhibitors target class I, class II, and/or class IV HDACs that govern cell proliferation, differentiation, migration, and angiogenesis. They inhibit angiogenesis through VEGF and hypoxia-inducible factor (24,25), affect class IIb HDAC–mediated cell migration, and induce class I HDAC–mediated cell apoptosis (26). Therefore, one should be cautious when using HDAC inhibitors to treat

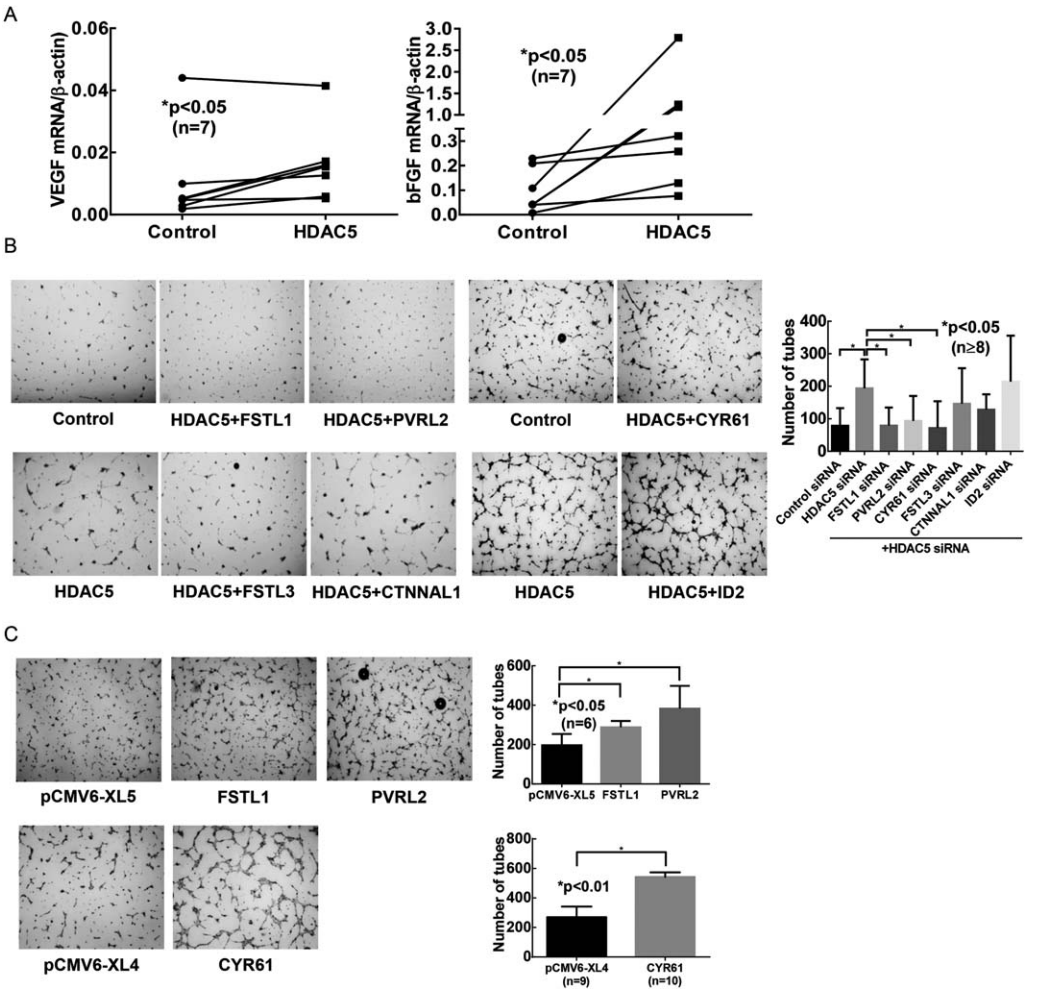

Figure 3. Promotion of tube formation by several up-regulated proangiogenic factors after *HDAC5* knockdown. **A,** Expression of vascular endothelial growth factor (VEGF) and basic fibroblast growth factor (bFGF) mRNA was determined by quantitative polymerase chain reaction in endothelial cells (ECs) from patients with systemic sclerosis (SSc) after treatment with *HDAC5* small interfering RNA (siRNA) or control siRNA. Increased expression after *HDAC5* knockdown was observed in both cases. **B,** Tube formation was assayed on Matrigel (left) and quantified as the number of tubes formed (right) after SSc ECs (n = 4 cell lines) were transfected with control siRNA, *HDAC5* siRNA, or *HDAC5* siRNA plus siRNA for the genes of interest. *FSTL1*, *PVRL2*, and *CYR61* appeared to play a key role in promoting angiogenesis after *HDAC5* knockdown, while *FSTL3*, *CTNNAL1*, and *ID2* did not. **C,** Induced overexpression of *FSTL1*, *PVRL2*, and *CYR61* resulted in increased tube formation by SSc ECs, as identified by Matrigel assay (left) and quantified as the number of tubes formed on Matrigel (right). Vectors pCMV6-XL5 and pCMV6-XL4 were used as controls. Results are the mean ± SD.

fibrosis in SSc, as this may be detrimental to the vasculopathic component of this disease.

Our results are consistent with those from a study by Urbich et al, who found that *HDAC5* knockdown led to an increase in tube formation by ECs on Matrigel (12). They also showed that the target genes regulated by *HDAC5* included *FGF2*, *SLIT2*, and *EPHB4*. We showed that bFGF (encoded by *FGF2*) was up-regulated after *HDAC5* knockdown (Figure 3A), and also identified additional genes that are repressed by *HDAC5*, including *PVRL2*, *FSTL1*, and *CYR61* (Table 3). The discrepancies between our study and the study by Urbich et al might be attributable to the different types of ECs used, and the methods that were applied to identify genes were also different (ATAC-seq versus oligonucleotide array).

Of note, in our study, the discrepancy between the mRNA expression levels of bFGF and VEGF and the ATAC-seq results may seem contradictory; however, it is not uncommon for chromatin accessibility and gene expression to lack correlation with each other. As shown in Table 3, only 8 of the 25 genes that showed a significant increase in chromatin accessibility had increased mRNA expression. These results point to the

importance of studying the epigenome and transcriptome simultaneously, because the integration of data obtained from both approaches would greatly facilitate the identification of target genes.

We identified several proangiogenic factors controlled by *HDAC5* (Table 3). *CYR61* (also known as CCN1) is a member of the CCN protein family that binds to the extracellular matrix and supports angiogenesis (27). In contrast to CCN2 (also known as connective tissue growth factor), which is profibrotic, *CYR61* is antifibrotic through activation of an integrin/oxidative stress–mediated pathway (28). Saigusa et al showed that *CYR61* is down-regulated in dermal small blood vessels of SSc patients compared to controls (29). We postulate that the antifibrotic nature of this molecule should also play a significant role in inhibiting the fibrotic process in SSc, since it has been shown that *CYR61* restricted fibrosis in several models of fibrosis, including the skin (28,30,31). However, the role of *CYR61* in SSc fibrosis awaits further investigation.

The role of *FSTL1* in fibrosis has mainly been observed in experimental studies of pulmonary fibrosis; depletion or blockade of *FSTL1* in mice attenuated bleomycin-induced lung fibrosis (32). However, contradictory results were obtained in a mouse model of renal fibrosis (33). Although our bioinformatics analysis showed that *FSTL1* played a role solely in fibrosis (Figure 2C), upon a more detailed literature search, we found that it is also involved in EC proliferation and tube formation (34). Although its role in SSc pathogenesis remains to be explored, it has been shown that *FSTL1* levels are elevated in SSc serum (35). In this study, we showed that the expression of *FSTL1* increased after *HDAC5* knockdown, a finding consistent with a previous study showing that *FSTL1* is regulated by histone acetylation (36).

PVRL2 is a cell adhesion molecule that connects to the actin cytoskeleton by binding to afadin (37). The mechanism by which nectin-2 promotes angiogenesis is not known. It is possible that it is mediated directly by its cell adhesion properties, but also indirectly through afadin, which promotes angiogenesis (38), or through interaction with other members of the adhesion molecule family (39). As adhesion molecules have been suggested to play a role in the pathogenesis of SSc (2), our finding that *PVRL2* improves the angiogenic ability of SSc ECs offers new insights into how these adhesion molecules are involved in this disease.

It appears that HDAC-5 also controls fibrosis through SSc ECs, as a few fibrotic genes, including *FSTL1*, *FSTL3*, and *SQSTM1*, were identified as being up-regulated after *HDAC5* knockdown in our study (Table 3). These genes are involved in both the TGFβ pathway (*FSTL1* and *FSTL3*) and the autophagy pathway (*SQSTM1*) (40,41). *FSTL3* also plays a role in angiogenesis through the inhibition of activin A (42,43). However, in our study, simultaneous knockdown of *HDAC5* and *FSTL3* did not reverse the angiogenic phenotype of SSc ECs. Although autophagy has been shown to play a role in various fibrotic disorders, including SSc (44,45), whether *SQSTM1* is critical warrants additional studies.

In addition to its role in angiogenesis, HDAC-5 appears to be involved in inflammation and immunity. It controls the inflammatory responses of macrophages and the functions of T cells (46,47). In addition, HDAC-5 negatively regulates chemokine and cytokine production in fibroblast-like synoviocytes in rheumatoid arthritis (48). Therefore, it is also possible that HDAC-5 has functional roles in the inflammatory and autoimmune aspect of SSc pathogenesis.

In conclusion, our results clearly show that epigenetic mechanisms contribute significantly to impaired angiogenesis in SSc. Increased expression of antiangiogenic *HDAC5* repressed several proangiogenic genes, resulting in dysregulated angiogenesis in SSc ECs. Coupling ATAC-seq with functional assays, we identified novel angiogenic and fibrotic genes that warrant additional studies to delineate their roles in the pathogenesis of SSc.

ACKNOWLEDGMENT

We thank Paul Renauer for his assistance in preparing figures for the manuscript.

AUTHOR CONTRIBUTIONS

All authors were involved in drafting the article or revising it critically for important intellectual content, and all authors approved the final version to be published. Dr. Sawalha had full access to all of the data in the study and takes responsibility for the integrity of the data and the accuracy of the data analysis.

Study conception and design. Tsou, Sawalha.
Acquisition of data. Tsou, Schiopu, Fox, Khanna, Sawalha.
Analysis and interpretation of data. Tsou, Wren, Amin, Sawalha.

REFERENCES

1. Steen VD, Medsger TA. Changes in causes of death in systemic sclerosis, 1972-2002. Ann Rheum Dis 2007;66:940–4.
2. Rabquer BJ, Koch AE. Angiogenesis and vasculopathy in systemic sclerosis: evolving concepts. Curr Rheumatol Rep 2012;14:56–63.
3. Mazzotta C, Romano E, Bruni C, Manetti M, Lepri G, Bellando-Randone S, et al. Plexin-D1/Semaphorin 3E pathway may contribute to dysregulation of vascular tone control and defective angiogenesis in systemic sclerosis. Arthritis Res Ther 2015;17:221.
4. Tsou PS, Rabquer BJ, Ohara RA, Stinson WA, Campbell PL, Amin MA, et al. Scleroderma dermal microvascular endothelial

cells exhibit defective response to pro-angiogenic chemokines. Rheumatology (Oxford) 2015;55:745–54.
5. Romano E, Chora I, Manetti M, Mazzotta C, Rosa I, Bellando-Randone S, et al. Decreased expression of neuropilin-1 as a novel key factor contributing to peripheral microvasculopathy and defective angiogenesis in systemic sclerosis. Ann Rheum Dis 2015;75:1541–9.
6. Tsou PS, Amin MA, Campbell P, Zakhem G, Balogh B, Edhayan G, et al. Activation of the thromboxane A2 receptor by 8-isoprostane inhibits the pro-angiogenic effect of vascular endothelial growth factor in scleroderma. J Invest Dermatol 2015;135:3153–62.
7. Manetti M, Guiducci S, Romano E, Ceccarelli C, Bellando-Randone S, Conforti ML, et al. Overexpression of VEGF165b, an inhibitory splice variant of vascular endothelial growth factor, leads to insufficient angiogenesis in patients with systemic sclerosis. Circ Res 2011;109:e14–26.
8. Ichimura Y, Asano Y, Akamata K, Takahashi T, Noda S, Taniguchi T, et al. Fli1 deficiency contributes to the suppression of endothelial CXCL5 expression in systemic sclerosis. Arch Dermatol Res 2014;306:331–8.
9. Serrati S, Chilla A, Laurenzana A, Margheri F, Giannoni E, Magnelli L, et al. Systemic sclerosis endothelial cells recruit and activate dermal fibroblasts by induction of a connective tissue growth factor (CCN2)/transforming growth factor β–dependent mesenchymal-to-mesenchymal transition. Arthritis Rheum 2013; 65:258–69.
10. Wang Y, Kahaleh B. Epigenetic repression of bone morphogenetic protein receptor II expression in scleroderma. J Cell Mol Med 2013;47:47–56.
11. Turtoi A, Peixoto P, Castronovo V, Bellahcene A. Histone deacetylases and cancer-associated angiogenesis: current understanding of the biology and clinical perspectives. Crit Rev Oncog 2015;20:119–37.
12. Urbich C, Rossig L, Kaluza D, Potente M, Boeckel JN, Knau A, et al. HDAC5 is a repressor of angiogenesis and determines the angiogenic gene expression pattern of endothelial cells. Blood 2009;113:5669–79.
13. Van den Hoogen F, Khanna D, Fransen J, Johnson SR, Baron M, Tyndall A, et al. 2013 classification criteria for systemic sclerosis: an American College of Rheumatology/European League Against Rheumatism collaborative initiative. Ann Rheum Dis 2013;72:1747–55.
14. Buenrostro JD, Giresi PG, Zaba LC, Chang HY, Greenleaf WJ. Transposition of native chromatin for fast and sensitive epigenomic profiling of open chromatin, DNA-binding proteins and nucleosome position. Nat Methods 2013;10:1213–8.
15. Li H, Durbin R. Fast and accurate short read alignment with Burrows-Wheeler transform. Bioinformatics 2009;25:1754–60.
16. Li H, Handsaker B, Wysoker A, Fennell T, Ruan J, Homer N, et al. The Sequence Alignment/Map format and SAMtools. Bioinformatics 2009;25:2078–9.
17. Zhang Y, Liu T, Meyer CA, Eeckhoute J, Johnson DS, Bernstein BE, et al. Model-based analysis of ChIP-Seq (MACS). Genome Biol 2008;9:R137.
18. Consortium EP. An integrated encyclopedia of DNA elements in the human genome. Nature 2012;489:57–74.
19. Shen L, Shao NY, Liu X, Maze I, Feng J, Nestler EJ. DiffReps: detecting differential chromatin modification sites from ChIP-seq data with biological replicates. PLoS One 2013;8:e65598.
20. Wren JD, Garner HR. Shared relationship analysis: ranking set cohesion and commonalities within a literature-derived relationship network. Bioinformatics 2004;20:191–8.
21. Ram O, Goren A, Amit I, Shoresh N, Yosef N, Ernst J, et al. Combinatorial patterning of chromatin regulators uncovered by genome-wide location analysis in human cells. Cell 2011;147:1628–39.
22. Huber LC, Distler JH, Moritz F, Hemmatazad H, Hauser T, Michel BA, et al. Trichostatin A prevents the accumulation of extracellular matrix in a mouse model of bleomycin-induced skin fibrosis. Arthritis Rheum 2007;56:2755–64.
23. Wang Y, Fan PS, Kahaleh B. Association between enhanced type I collagen expression and epigenetic repression of the FLI1 gene in scleroderma fibroblasts. Arthritis Rheum 2006;54:2271–9.
24. Deroanne CF, Bonjean K, Servotte S, Devy L, Colige A, Clausse N, et al. Histone deacetylases inhibitors as anti-angiogenic agents altering vascular endothelial growth factor signaling. Oncogene 2002;21:427–36.
25. Kim SH, Jeong JW, Park JA, Lee JW, Seo JH, Jung BK, et al. Regulation of the HIF-1α stability by histone deacetylases. Oncol Rep 2007;17:647–51.
26. Khan O, la Thangue NB. HDAC inhibitors in cancer biology: emerging mechanisms and clinical applications. Immunol Cell Biol 2012;90:85–94.
27. Jun JI, Lau LF. Taking aim at the extracellular matrix: CCN proteins as emerging therapeutic targets. Nat Rev Drug Discov 2011;10:945–63.
28. Jun JI, Lau LF. The matricellular protein CCN1 induces fibroblast senescence and restricts fibrosis in cutaneous wound healing. Nat Cell Biol 2010;12:676–85.
29. Saigusa R, Asano Y, Taniguchi T, Yamashita T, Takahashi T, Ichimura Y, et al. A possible contribution of endothelial CCN1 downregulation due to Fli1 deficiency to the development of digital ulcers in systemic sclerosis. Exp Dermatol 2015;24:127–32.
30. Kim KH, Chen CC, Monzon RI, Lau LF. Matricellular protein CCN1 promotes regression of liver fibrosis through induction of cellular senescence in hepatic myofibroblasts. Mol Cell Biol 2013;33:2078–90.
31. Qin Z, Fisher GJ, Quan T. Cysteine-rich protein 61 (CCN1) domain-specific stimulation of matrix metalloproteinase-1 expression through $\alpha V\beta 3$ integrin in human skin fibroblasts. J Biol Chem 2013;288:12386–94.
32. Dong Y, Geng Y, Li L, Li X, Yan X, Fang Y, et al. Blocking follistatin-like 1 attenuates bleomycin-induced pulmonary fibrosis in mice. J Exp Med 2015;212:235–52.
33. Hayakawa S, Ohashi K, Shibata R, Kataoka Y, Miyabe M, Enomoto T, et al. Cardiac myocyte-derived follistatin-like 1 prevents renal injury in a subtotal nephrectomy model. J Am Soc Nephrol 2015;26:636–46.
34. Ouchi N, Asaumi Y, Ohashi K, Higuchi A, Sono-Romanelli S, Oshima Y, et al. DIP2A functions as a FSTL1 receptor. J Biol Chem 2010;285:7127–34.
35. Li D, Wang Y, Xu N, Wei Q, Wu M, Li X, et al. Follistatin-like protein 1 is elevated in systemic autoimmune diseases and correlated with disease activity in patients with rheumatoid arthritis. Arthritis Res Ther 2011;13:R17.
36. Zhao W, Han HB, Zhang ZQ. Suppression of lung cancer cell invasion and metastasis by connexin43 involves the secretion of follistatin-like 1 mediated via histone acetylation. Int J Biochem Cell Biol 2011;43:1459–68.
37. Takai Y, Irie K, Shimizu K, Sakisaka T, Ikeda W. Nectins and nectin-like molecules: roles in cell adhesion, migration, and polarization. Cancer Sci 2003;94:655–67.
38. Tawa H, Rikitake Y, Takahashi M, Amano H, Miyata M, Satomi-Kobayashi S, et al. Role of afadin in vascular endothelial growth factor- and sphingosine 1-phosphate-induced angiogenesis. Circ Res 2010;106:1731–42.
39. Fukuhara A, Irie K, Nakanishi H, Takekuni K, Kawakatsu T, Ikeda W, et al. Involvement of nectin in the localization of junctional adhesion molecule at tight junctions. Oncogene 2002;21: 7642–55.
40. Sidis Y, Tortoriello DV, Holmes WE, Pan Y, Keutmann HT, Schneyer AL. Follistatin-related protein and follistatin differentially neutralize endogenous vs. exogenous activin. Endocrinology 2002; 143:1613–24.
41. Panse KD, Felkin LE, Lopez-Olaneta MM, Gomez-Salinero J, Villalba M, Munoz L, et al. Follistatin-like 3 mediates paracrine fibroblast activation by cardiomyocytes. J Cardiovasc Transl Res 2012;5:814–26.

42. Wankell M, Kaesler S, Zhang YQ, Florence C, Werner S, Duan R. The activin binding proteins follistatin and follistatin-related protein are differentially regulated in vitro and during cutaneous wound repair. J Endocrinol 2001;171:385–95.
43. Robertson R, Mahmood W, McGonnell I, Mukherjee A. Follistatin-like 3 (FSTL3), a transforming growth factor β ligand inhibitor, is essential for placental development in mice. Endocrine Abstracts 2013;31:OC3.6.
44. Del Principe D, Lista P, Malorni W, Giammarioli AM. Fibroblast autophagy in fibrotic disorders. J Pathol 2013;229:208–20.
45. Dumit VI, Kuttner V, Kappler J, Piera-Velazquez S, Jimenez SA, Bruckner-Tuderman L, et al. Altered MCM protein levels and autophagic flux in aged and systemic sclerosis dermal fibroblasts. J Invest Dermatol 2014;134:2321–30.
46. Xiao H, Jiao J, Wang L, O'Brien S, Newick K, Wang LC, et al. HDAC5 controls the functions of Foxp3(+) T-regulatory and CD8(+) T cells. Int J Cancer 2016;138:2477–86.
47. Poralla L, Stroh T, Erben U, Sittig M, Liebig S, Siegmund B, et al. Histone deacetylase 5 regulates the inflammatory response of macrophages. J Cell Mol Med 2015;19:2162–71.
48. Angiolilli C, Grabiec AM, Ferguson BS, Ospelt C, Malvar Fernandez B, van Es IE, et al. Inflammatory cytokines epigenetically regulate rheumatoid arthritis fibroblast-like synoviocyte activation by suppressing HDAC5 expression. Ann Rheum Dis 2016;75:430–8.